Studies of the Electronic Structure of Metallocene-Based Second-Order Nonlinear Optical Dyes

Stephen Barlow,[†] Heather E. Bunting,[‡] Catherine Ringham,[‡] Jennifer C. Green,[‡] Gerold U. Bublitz,[#] Steven G. Boxer,[#] Joseph W. Perry,[§] and Seth R. Marder*[,§]

Contribution from the Beckman Institute, 139-74, California Institute of Technology, Pasadena, California 91125, Inorganic Chemistry Laboratory, University of Oxford, South Parks Road, Oxford, OX1 3QR, UK, Department of Chemistry, Stanford University, Stanford, California 94305-5080, Jet Propulsion Laboratory, California Institute of Technology, Pasadena, California 91109, and Department of Chemistry, University of Arizona, Tucson, Arizona 85721

Received August 27, 1998

Abstract: This paper describes a simple orbital picture for understanding the optical transitions and the second-order nonlinear optical response of metallocene-based chromophores of the form metallocene−(π-bridge)−acceptor, and experimental studies to test this model. From a combination of UV photoelectron spectroscopy, cyclic voltammetry, and density functional calculations, it is deduced that the three highest occupied orbitals are little perturbed from the parent metallocenes, that the HOMO-3 is a π-orbital delocalized between the metallocene cyclopentadienyl ring and the unsaturated bridge, and that the LUMO is acceptor based. The lowest energy transition in the UV/visible/near-IR spectra of these compounds is assigned to a metal-to-acceptor transition, while the higher energy transition is attributed to a transition to the acceptor-based LUMO from the delocalized HOMO-3 orbital. The variations in oscillator strength can be rationalized by considering the low-energy transition as borrowing intensity from the high-energy transition. Stark spectroscopy confirms that large dipole moment changes are associated with both transitions, as expected from our assignment. These dipole moment changes indicate that, according to the perturbation theory-derived expression for the first hyperpolarizability, β, both transitions contribute significantly to the observed optical nonlinearity.

Introduction

There has been considerable interest in the second-order nonlinear optical (NLO) properties of organometallic chromophores.[1−3] Powder second harmonic generation (SHG) efficiencies 62 and 220 times that of urea were found for *Z*-1-ferrocenyl-2-(*p*-nitrophenyl)ethylene, **Fc[1]1** (Figure 1),[4] and *E*-1-ferrocenyl-2-(*N*-methylpyridinium-4-yl)ethylene iodide, **Fc[1]3-I** (Figure 1),[5] respectively. These properties arise from the combination of moderate molecular first hyperpolarizabilities, β, with noncentrosymmetric crystal structures. More recent studies of metallocene-based chromophores have focused on the determination and understanding of molecular properties, especially using electric field induced second harmonic generation (EFISH).[6−13] EFISH yields values of $\mu\beta$, the vectorial projection of the hyperpolarizability along the molecular dipole moment direction; $\mu\beta$ is also a figure of merit for the NLO behavior of materials rendered noncentrosymmetric by poling chromophores in a polymer matrix. Ferrocene derivatives with very large values of $\mu\beta$, comparable with the best all-organic chromophores, are now known; 11200 × 10^{-48} esu for **Fc[4]6** (Figure 2a)[12] vs 15000 × 10^{-48} esu for **1** (Figure 2b).[14,15]

The two-level model[16,17] relates the static molecular hyperpolarizability, $\beta(0)$, to characteristics of the molecule's optical

* To whom correspondence should be addressed at the University of Arizona.

† Beckman Institute. Present address: Inorganic Chemistry Laboratory.

‡ Inorganic Chemistry Laboratory.

Stanford University.

§ Beckman Institute, Jet Propulsion Lab, and University of Arizona.

(1) Marder, S. R. In *Inorganic Materials*, 2nd ed.; Bruce, D. W., O'Hare, D., Eds.; Wiley: Chichester, 1996, and references therein.

(2) Long, N. J. *Angew. Chem., Int. Ed. Engl.* **1995**, *34*, 21−38 and references therein.

(3) Verbiest, T.; Houbrechts, S.; Kauranen, M.; Clays, K.; Persoons, A. *J. Mater. Chem.* **1997**, *7*, 2175−2189 and references therein.

(4) Green, M. L. H.; Marder, S. R.; Thompson, M. E.; Bandy, J. A.; Bloor, D.; Kolinsky, P. V.; Jones, R. J. *Nature* **1987**, *330*, 360−362.

(5) Marder, S. R.; Perry, J. W.; Schaefer, W. P.; Tiemann, B. G. *Organometallics* **1991**, *10*, 1896−1901.

(6) Calabrese, J. C.; Cheng, L.-T.; Green, J. C.; Marder, S. R.; Tam, W. *J. Am. Chem. Soc.* **1991**, *113*, 7227−7232.

(7) Doisneau, G.; Balavoine, G.; Fillebeen-Khan, T.; Clinet, J.-C.; Delaire, J.; Ledoux, I.; Loucif, R.; Pucetti, G. *J. Organomet. Chem.* **1991**, *1991*, 299−304.

(8) Loucif-Saïbi, R.; Delaire, J. A.; Bonazzola, L.; Doisneau, G.; Balavoine, G.; Fillebeen-Khan, T.; Ledoux, I.; Puccetti, G. *Chem. Phys.* **1992**, *167*, 369−375.

(9) Yuan, Z.; Taylor, N. J.; Sun, Y.; Marder, T. B.; Williams, I. D.; Cheng, L.-T. *J. Organomet. Chem.* **1993**, *449*, 27−37.

(10) Blanchard-Desce, M.; Runser, C.; Fort, A.; Barzoukas, M.; Lehn, J.-M.; Bloy, V.; Alain, V. *Chem. Phys.* **1995**, *199*, 253−261.

(11) Alain, V.; Blanchard-Desce, M.; Chen, C. T.; Marder, S. R.; Fort, A.; Barzoukas, M. *Synth. Met.* **1996**, *81*, 133−136.

(12) Alain, V.; Fort, A.; Barzoukas, M.; Chen, C. T.; Blanchard-Desce, M.; Marder, S. R.; Perry, J. W. *Inorg. Chim. Acta* **1996**, *242*, 43.

(13) Alagesan, K.; Chandra-Ray, P.; Kumar-Das, P.; Samuleson, A. G. *Curr. Sci.* **1996**, *70*, 69−71.

(14) Ahlheim, M.; Barzoukas, M.; Bedworth, P. V.; Blanchard-Desce, M.; Fort, A.; Hu, Z.-Y.; Marder, S. R.; Perry, J. W.; Runser, C.; Staehelin, M.; Zysset, B. *Science* **1996**, *271*, 335−337.

(15) These $\mu\beta(2\omega)$ values were obtained by EFISH at 1.907 μm in chloroform (**Fc″[4]6**) or dichloromethane (**1**). The dispersion-corrected $\mu\beta(0)$ values are substantially lower: a value of 5000 × 10^{-48} esu is estimated for **1**.

(16) Oudar, J. L.; Chemla, D. S. *J. Chem. Phys.* **1977**, *66*, 2664−2668.

(17) Oudar, J. L. *J. Chem. Phys.* **1977**, *67*, 446−457.

10.1021/ja9830896 CCC: $18.00
Published on Web 04/02/1999

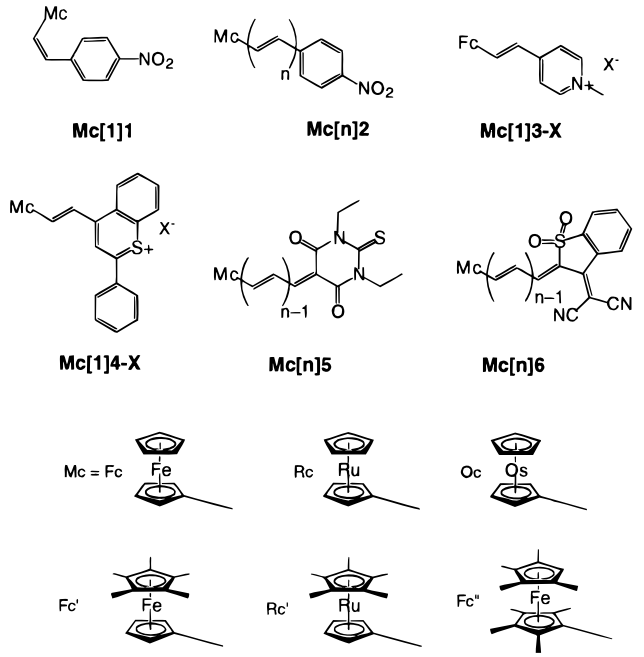

Figure 1. Structures of metallocene-based NLO chromophores discussed in this work.

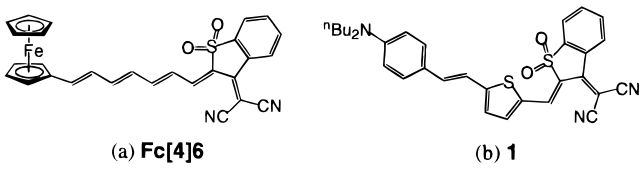

$\mu\beta(2\omega) = 11200 \times 10^{-48}$ esu

$\mu\beta(2\omega) = 15000 \times 10^{-48}$ esu

$\mu\beta(0) = 5000 \times 10^{-48}$ esu

Figure 2. Structures of highly efficient (a) organometallic[12] and (b) organic[14] NLO chromophores, together with $\mu\beta(2\omega)$ values determined by EFISH at 1.907 μm in chloroform (**Fc[4]6**) or dichloromethane (**1**). The dispersion-corrected static $\mu\beta(0)$ value for **1** was estimated by using the two-level model.[17]

transitions through the equation:

$$\beta(0) \propto (\mu_{ee} - \mu_{gg})\frac{\mu_{ge}^2}{E_{ge}^2} \qquad (1)$$

where μ_{ee} and μ_{gg} are excited and ground-state dipole moments, respectively, μ_{ge} is the transition dipole moment, and E_{ge} is the transition energy. Thus, to a first approximation, trends in β can be inferred from knowledge of these parameters. Molecules with intense low-energy charge-transfer transitions will have large β.

In the case of organic donor−acceptor dyes such as *E*-4-(dimethylamino)-4′-nitrostilbene, a single low-energy charge-transfer transition is observed and dominates the NLO response.[17] However, the ultraviolet/visible/near-infrared (UV−vis−NIR) spectra of analogous molecules with metallocene donors show *two* low-energy transitions. To develop design guidelines for metallocene dyes, it is helpful to know which transitions contribute significantly to the NLO response and to understand the molecular origin of these transitions. We previously suggested assignments for the two transitions (model I) based upon the spectral trends observed with variation of chromophore structure, and upon extended Hückel calculations for **Fc[1]2**.[6] In this model, the highest occupied orbitals were the essentially nonbonding $d_{z^2}/d_{x^2-y^2}/d_{xy}$ orbitals of the metal (**M**), while the next highest orbital (HOMO-3, π) had mainly cyclopentadienyl and conjugated bridge, with little metal, character. The LUMO (**A**) was localized on the acceptor, while higher in energy was an orbital (LUMO+1) largely localized on the conjugated bridge, but with a small degree of acceptor and metal d character, hereafter referred to as π^*. The lower energy (LE) of the two transitions was assigned to a charge-transfer transition between the HOMO and the bridge-localized LUMO+1; the possibility of a direct HOMO−LUMO transition was considered less likely owing to the small spatial overlap between these orbitals. The higher energy (HE) transition was assigned to a transition from π to LUMO. The substantial dipole moment changes expected for both transitions, together with their low energies and high oscillator strengths, suggested *both* transitions should contribute to the observed NLO response. A more quantitative analysis of the spectra of these compounds was described by Kanis, Ratner, and Marks,[18−20] using Zerner intermediate neglect of differential overlap (ZINDO) calculations. The calculations were able to predict the energies of the HE transitions for a series of ferrocene derivatives within 0.3 eV, but were somewhat less accurate in predicting the energies of the LE transitions (a discrepancy of ca. 0.8 eV being obtained between calculation and experiment for **Fc[1]1**) and consistently significantly underestimated the intensities of the LE transitions. Sum over states (SOS) calculation of β gave rather good agreement with experiment. The LE transition was assigned as a metal-localized ligand-field (d−d) transition with little contribution to β, while the HE transition was identified as the major contributor to β and was described as a metal−acceptor transition. Hereafter, these assignments are referred to as model II. The previous assignments discussed above (models I and II) are approximations of the true electron redistributions associated with the two transitions. Such a simplified model is useful if it allows one to develop a chemically intuitive picture of the relationship between a chromophore's structure and its linear and nonlinear optical properties, and if the model has predictive power. Full computation of the optical properties of this class of molecules would be interesting; however, accurate reproduction of the *linear* optical properties of these molecules has not been achieved with any computational method.

Recently, additional examples of metallocene−bridge−acceptor dyes have been synthesized;[11,12] these have greater structural variation than within the series available when models I and II were proposed, and, most notably, include molecules with considerably stronger acceptor groups. Neither model I nor II is fully satisfactory in rationalizing the observed spectral trends in this expanded class of metallocene dyes. We have, therefore, attempted to develop a more refined description of the transitions (model III), building upon models I and II. Here we describe model III and compare its predictions with observed trends in UV−vis−NIR spectra. We also present additional data—photoelectron spectroscopy, electrochemistry, and Stark spectroscopy—for both previously reported and new compounds, which are consistent with model III and which yield additional insight into the orbital structure of metallocene−(π-bridge)−acceptor chromophores, and thus, into the origin of the NLO response of this class of compounds.

(18) Kanis, D. R.; Ratner, M. A.; Marks, T. J. *J. Am. Chem. Soc.* **1990**, *112*, 8203−8204.
(19) Kanis, D. R.; Ratner, M. A.; Marks, T. J. *J. Am. Chem. Soc.* **1992**, *114*, 10338−10357.
(20) Kanis, D. R.; Ratner, M. A.; Marks, T. J. *Chem. Rev.* **1994**, *94*, 195−242.

Table 1. Ionization Energies (eV) for *p*-Nitrostyrene

assignment	π_4	π_3	π_2	NO_2						
I.E.	9.29	10.05	10.75	11.15	12.42	12.86	13.8	14.8	15.6	16.5

Results and Discussion

Model for the Origin of the Spectra. The spectroscopic properties of this class of molecules can largely be accounted for as follows. The highest occupied molecular orbitals correspond to the predominately nonbonding, nearly degenerate $d_{z^2}/d_{x^2-y^2}/d_{xy}$ orbitals (**M**) of the metal. The next highest orbital (HOMO-3, π) is formed from a combination of the highest occupied cyclopentadienyl orbital and the highest occupied π-bridge orbital. The LUMO (which we will refer to as **A**) is largely localized on the acceptor, but also has a small bridge contribution. The LE absorption is a **M**→**A** transition, while the HE absorption is a π→**A** transition.[21] The assignment of the HE transition is, therefore, equivalent to that in model I, but the present model differs in the identification of the acceptor orbital of the LE transition. Model I invoked the π-bridge based LUMO+1, owing to the low spatial overlap between **M** and **A**; however, some of the spectral data (vide infra) are in conflict with that assignment while the observed intensities may be accounted for in terms of "intensity borrowing". Specifically, mixing of the π→**A** excited state (e') into the ground state (g) and mixing between **M**→**A** (e) and π→**A** (e') excited states allows both ground and **M**→**A** states to gain bridge character and thus experience greater spatial overlap with one another. Perturbation theory dictates that the degree of this mixing, and hence the **M**→**A** oscillator strength, will depend inversely upon the energetic separations between the ground and π→**A** excited state, $\Delta E_{ge'}$, and between the **M**→**A** and π→**A** excited states, $\Delta E_{ee'}$. Thus, it should be possible to use the present model (model III) to make qualitative predictions of trends in both transition energies and transition intensities.

Kanis, Ratner, and Marks also suggested that the LE transition could borrow intensity from the HE transition and that neglect of the vibrational coupling responsible for this borrowing in the ZINDO calculations could account for the underestimation of the LE transition intensity. In their model (model II) this corresponds to a d−d transition borrowing **M**→**A** character; in contrast, the present model (model III) considers a **M**→**A** transition borrowing from a π→**A** transition.

The three models are summarized pictorially for **Mc[1]2** in Figure 3. In the following sections we present experimental evidence in support of model III. The structures of the compounds discussed are shown in Figure 1; the compounds were prepared as described previously,[4−6,11,12,22,23] or as described in the Supporting Information.

UV Photoelectron Spectroscopy (UV-PES). He I and He II photoelectron (PE) spectra were recorded for **Fc[1]1**, **Fc[1]2**, **Rc[1]1**, and **Oc[1]2**, together with the model compound *p*-nitrostyrene. The ionizations observed for *p*-nitrostyrene are summarized in Table 1,[24] together with assignments made by comparison with the PE spectra of styrene[25] and nitrobenzene.[26]

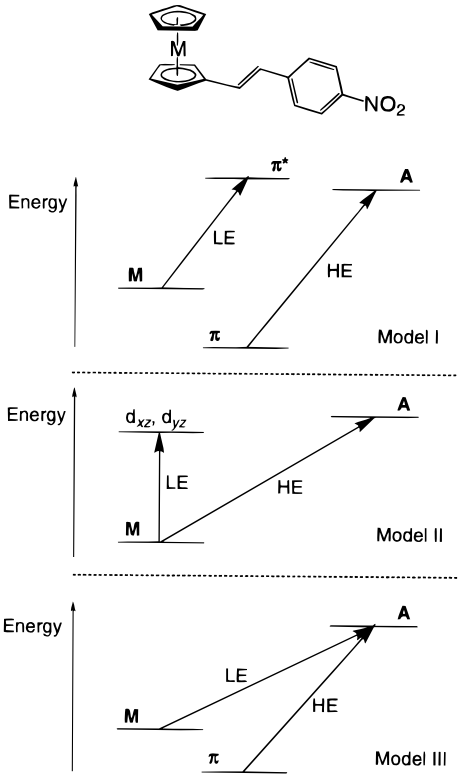

Figure 3. Schematic representation of the orbitals identified by the three models as most important in the low (LE) and high (HE) energy transitions for the spectra of metallocene−(π-bridge)−acceptor chromophores. The horizontal scale represents the approximate spatial location of the orbitals along the molecule.

The spectra of the metallocene−bridge−acceptor dyes (Figure 4; Table 2)[24] can be assigned by comparison with the spectra of *p*-nitrostyrene and the appropriate parent metallocenes.[27−29] The lowest energy ionizations of metallocenes correspond to removal of electrons from the occupied $d_{x^2-y^2}/d_{xy}$ (e_2') and d_{z^2} (a_1') orbitals. For ferrocene two distinct transitions are observed, while in ruthenocene the energy difference cannot be resolved and in osmocene three transitions are seen owing to spin−orbit splitting of the $^2E_2$ ion state. The lowest energy ionizations, A, for the 1-metallocenyl-2-(*p*-nitrophenyl)ethylenes closely resemble those of the respective parent metallocenes, both in terms of the splitting of the bands and their relative enhancement in the He II spectra, but are all shifted by ca. 0.1 eV to higher energy. The magnitude of this shift, coupled with the constant splittings, suggests very little perturbation of the d-levels by the substituent, i.e., that the HOMO in these molecules can be regarded as metal-based.

The next lowest ionization energy (IE) band in the parent unsubstituted metallocenes is due to ionization of the e_1' orbitals; these are a combination of the e_1 orbitals of the two cyclopentadienyl rings, possibly with some contribution from the p_x and p_y orbitals of the metal. The variation in the IE of this band between ferrocene, ruthenocene, and osmocene is much less than

(21) We also expect d−d transitions to be present in the visible part of the spectrum. However, we expect these to be very weak compared to the two charge-transfer transitions and to make negligible contribution to the observed optical nonlinearity. Therefore, they are not considered further in our discussion.

(22) Toma, S.; Gáplovsky, A.; Elecko, P. *Chem. Pap.* **1985**, *39*, 115−124.

(23) Bunting, H. E.; Green, M. L. H.; Marder, S. R.; Thompson, M. E.; Bloor, D.; Kolinsky, P. V.; Jones, R. J. *Polyhedron* **1992**, *11*, 1489−1499.

(24) He I and He II PE spectra for *p*-nitrostyrene, **Fc[1]1**, **Fc[1]2**, **Rc[1]1**, and **Oc[1]2** are presented as Supporting Information.

(25) Rabalais, J. W.; Colton, R. J. *J. Electron Spectrosc.* **1972**, *1*, 83.

(26) Rabalais, J. W. *J. Chem. Phys.* **1972**, *57*, 960.

(27) Evans, S.; Green, M. L. H.; Jewitt, B.; Orchard, A. F.; Pygall, C. F. *J. Chem. Soc., Faraday Trans. 2* **1972**, *68*, 1847−1865.

(28) Cauletti, C.; Green, J. C.; Kelly, M. R.; Robbins, J.; Smart, J. C. *J. Electron Spectrosc. Rel. Phenom.* **1980**, *19*, 327−353.

(29) Cooper, G.; Green, J. C.; Payne, M. P. *Mol. Phys.* **1988**, *63*, 1031.

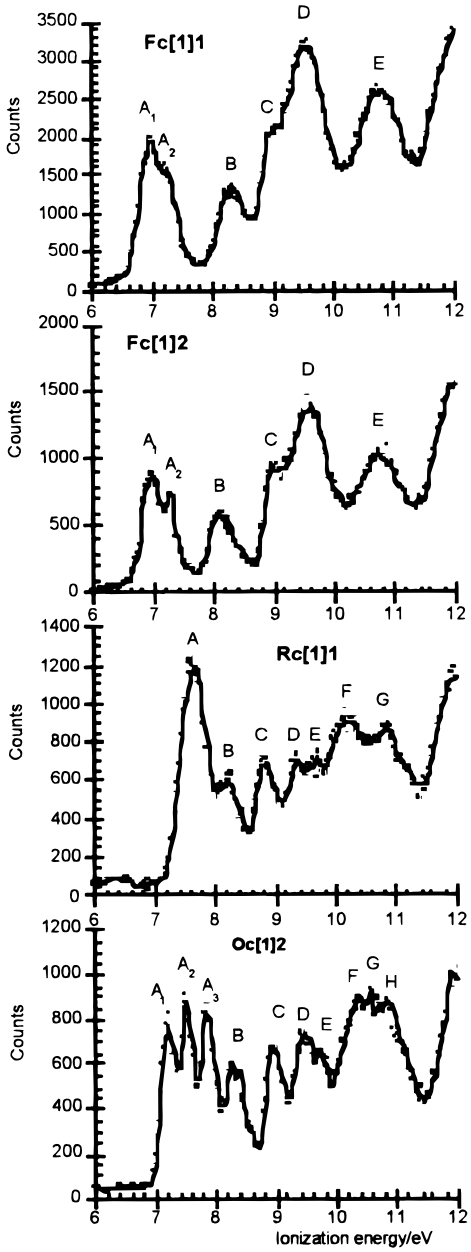

Figure 4. He I photoelectron spectra of *Z*-1-ferrocenyl-2-(*p*-nitrophenyl)ethylene, **Fc[1]1**, *E*-1-ferrocenyl-2-(*p*-nitrophenyl)ethylene, **Fc[1]2**, *Z*-1-ruthenocenyl-2-(*p*-nitrophenyl)ethylene, **Rc[1]1**, and *E*-1-osmocenyl-2-(*p*-nitrophenyl)ethylene, **Oc[1]2**.

Table 2. Ionization Energies (eV) for Four Metallocene-Based NLO Chromophores

Fc[1]1	Fc[1]2	Rc[1]1	Oc[1]2	assignment
6.98 A_1	6.97 A_1	7.57 A	7.22 A_1	$d_{z^2}/d_{x^2-y^2}/d_x$
7.26 A_2	7.31 A_2		7.50 A_2	
			7.85 A_3	
8.36 B	8.20 B	8.15 B	8.30 B	$e_1' - \pi_4$
9.08 C	9.05 C	8.72 C	8.96 C	e_1'
9.59 D	9.56 D	9.30 D	9.47 D	$e_1' + \pi_4$
		9.70 E	9.69 E	π_3
		10.15 F	10.32 F	e_1''
			10.58 G	e_1''
10.76 E	10.79 E	10.82 G	10.82 H	NO_2
12.98	12.7	12.4	12.6	
13.5	13.7	13.6	13.8	
16.6	16.6	16.5	17.0	

the variation in the $d_{x^2-y^2}/d_{xy}/d_{z^2}$ band IE. The other combination of the ring e_1 orbitals can combine with the metal d_{xz}/d_{yz} orbitals to give the e_1'' orbitals associated with the next band in the metallocene spectra. The IE of the e_1'' band increases substantially as the metal is changed from iron to ruthenium to osmium. The PE spectra of the nitrostyrene metallocene derivatives all show a band, B, at ca. 8.3 eV. This band cannot be accounted for by the superposition of the spectrum of the appropriate metallocene, where the e_1' ionizations occur in the range 8.51−8.72 eV, and that of *p*-nitrostyrene, the lowest energy ionization of which is at 9.29 eV. Thus, the presence of the nitrostyrene substituent leads to a substantial perturbation of the metallocene electronic structure. We assign band B to an orbital resulting from an antibonding combination of the HOMO of *p*-nitrostyrene and one of the pair of e_1' orbitals on the cyclopentadienyl ring to which the substituent is bound. Band B shows no relative intensity increase in the He II spectra, indicating that the corresponding orbital has little metal d-character. The variation in the energy of band B ionizations between iron, ruthenium, and osmium mirrors that in the e_1' ionizations of the parent metallocenes and is small relative to the variation in the band A IEs.[30] Therefore, the PES provides evidence for the delocalized orbital (labeled π), which in model III is the donor orbital in the HE optical transition (vide supra). The assignments of the remaining bands are summarized in Table 2.

Density functional (DF) calculations were carried out for **Fc[1]1** and **Fc[1]2** (using the Amsterdam Density Functional package version 2.3.[31]) in order to provide an independent orbital picture for these compounds, thus helping us to determine the validity of the orbital picture deduced above from the PE spectra. The orbital structure given by the DFT calculation is similar to that previously produced with extended Hückel calculations.[6] The HOMO is largely localized on the metal, as are the HOMO-1 and the HOMO-2, while the HOMO-3 has the delocalized π structure inferred from the position of band B in the PE spectrum. Iso-surfaces for the HOMO-3 and the principally acceptor-based LUMO of **Fc[1]2** are shown in Figure 5. The ionization energies for the HOMO and HOMO-3 of **Fc[1]2** were calculated explicitly by the ΔSCF method. The values found were 7.0 and 7.7 eV, in good agreement with the experimental values of 7.0 and 8.2 eV, respectively.

In summary, the most important results from UV−PES are as follows. First, the three highest occupied orbitals of the 1-metallocenyl-2-(*p*-nitrophenyl)ethylenes are similar to those of the appropriate parent metallocenes. Second, these molecules have a π-orbital that is delocalized over the cyclopentadienyl ring and the π-bridge, which is higher in energy than either the highest occupied cyclopentadienyl-based orbitals of the parent metallocene or the HOMO of *p*-nitrostyrene, and which is relatively unaffected by the identity of the metal.

Electrochemistry. Electrochemistry offers the possibility to examine trends in LUMO energies, as well as providing an alternative probe to the UV−PES of the trends in HOMO energies. We studied a range of metallocene−(π-bridge)−acceptor compounds using cyclic voltammetry in tetrahydrofuran (0.1 M $[^nBu_4N]^+[PF_6]^-$). Processes attributable to the $[m]^+/[m]$ couple, as reversible as the ferrocenium/ferrocene couple under the same conditions, were observed for all the ferrocenyl and octamethylferrocenyl compounds studied. Ruthenocene itself

(30) Interestingly, the PE spectra of **Fc[1]1** and **Fc[1]2** are virtually superimposable, except that band B occurs at lower IE in the *E*-isomer, **Fc[1]2**. This effect can be attributed to the nonplanar π-system of the *Z*-isomer leading to a weaker interaction between cyclopentadienyl and *p*-nitrostyrene π-orbitals; this nonplanarity is evident in the crystal structure reported in ref 4.

(31) Baerends, E. J.; te Velde, G. ADF, version 2.0.1; Department of Theoretical Chemistry, Vrije Universiteit, Amsterdam, 1996.

Table 3. Half-Wave Potentials (in mV) vs Ferrocenium/Ferrocene for Selected Metallocene-Containing Chromophores, Measured with Use of Cyclic Voltammetry in THF (0.1 M $[^nBu_4N]^+[PF_6]^-$)

	Mc[*n*]2		**Mc[*n*]5**	**Mc[*n*]6**		**Mc[1]3-Cl**
	$E_{1/2}([m]^+/[m])$	$E_{1/2}([m]/[m]^-)$	$E_{1/2}([m]^+/[m])$	$E_{1/2}([m]^+/[m])$	$E_{1/2}([m]/[m]^-)$	$E_{1/2}([m]^+/[m])$
Fc, *n* = 1	+25	−1670	+260	+325	−1090	+85
Fc, *n* = 2	+25	−1635	+180	+200	−950	
Fc, *n* = 3			+95	+110	−880	
Fc″, *n* = 1	−270	−1685				
Fc″, *n* = 3			−205	−183	−960	
Rc, *n* = 1	*a*	−1665				
Rc, *n* = 3			*a*	*a*	−880	

[a] Irreversible.

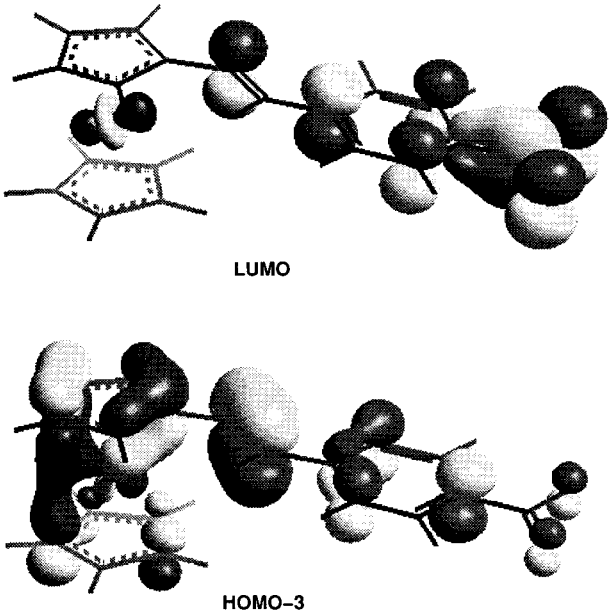

Figure 5. Representations of the HOMO-3 and the LUMO of **Fc[1]2** according to DF calculations.

shows an electrochemically irreversible two-electron oxidation;[32] the ruthenocenyl dyes also showed no reversible process assignable to the $[m]^+/[m]$ couple. The compounds with *p*-nitrophenyl acceptors (**Mc[*n*]2** series) all showed features attributable to the $[m]/[m]^-$ couple with reversibility comparable to that of ferrocenium/ferrocene, while compounds with *N*,*N*′-diethylthiobarbituric acid acceptors (**Mc[*n*]5** series) showed irreversible $[m]/[m]^{n-}$ processes; no reversible molecular reduction was observed for **Fc[1]3-Cl**. The $[m]/[m]^-$ features for the **Mc[*n*]6** series were characteristic of situations in which the electron transfer itself is reversible, but where the reduced species undergoes a chemical reaction on a time scale comparable with that of the electron transfer.[33,34] Half wave potentials are summarized in Table 3.

In the series **Mc[*n*]2**, the potentials for the $[m]/[m]^-$ couple occur in the range −1635 to −1685 mV; $[m]/[m]^-$ potentials of −1670 and −1730 mV were found, under the same conditions, for the model compounds *p*-nitrostyrene[35] and nitrobenzene, respectively. These data suggest a LUMO that is largely localized on the nitrophenyl group, with some contribution from the π-bridge, and thus, consistent with model III and with the results of DF calculations (Figure 5). **Fc[2]2** is slightly easier to reduce than **Fc[1]2**, indicative of a larger bridge contribution in the more extended species where empty bridge-based and acceptor-based orbitals will be closer in energy, leading to a stronger in-phase interaction and, thus, to a lower energy LUMO. Recently the ESR spectrum of the **Fc[1]2** radical anion has been reported.[36] The hyperfine coupling clearly shows the unpaired electron to be largely localized on the nitrophenyl ring, also consistent with **Fc[1]2** having a nitrobenzene-like LUMO.[37]

The $[m]^+/[m]$ couples for **Fc[1]2** and **Fc[2]2** occur at experimentally identical potential, +25 mV vs ferrocene (a single methyl substituent would have a somewhat larger effect of ca. 55 mV[38]), implying the HOMO to be principally localized on the ferrocene moiety and having even less π-character than the LUMO. This result is clearly consistent with the UV−PES and DF results discussed above. The $[m]^+/[m]$ couples for *E*-4-Fc-C_6H_4-CH=CH-C_6H_4-4-NO_2 and 4-Fc-C_6H_4-N=N-C_6H_4-4-NO_2 have been previously reported to be +20 and +70 mV, respectively, vs ferrocene in CH_2Cl_2.[39] The octamethylferrocenyl complex, **Fc″[1]2**, is considerably easier to oxidize than its ferrocene analogue, consistent with the well-known effect of methylation upon ferrocene oxidation potentials.[38,40−42]

For compounds with stronger acceptors (**Mc[*n*]5** and **Mc[*n*]6**) the trends in redox behavior are more complex due to more effective coupling of donor and acceptor in these compounds, the degree of coupling decreasing with increasing bridge length. This coupling is equivalent to the incorporation of more charge-transfer character into the ground state of the molecule, equivalent to increased contributions to the ground state from resonance structures such as those shown in the right-hand portion of Figure 6.[43]

UV−Vis−NIR Spectra. Trends in UV−vis−NIR spectra have been reported previously for a number of compounds. Here we compare qualitative predictions based upon the three models with these results and with additional data. We will examine in turn the effect of changing acceptor strength, changing the

(32) Diaz, A. F.; Mueller-Westerhoff, U. T.; Nazzar, A.; Tanner, M. *J. Organomet. Chem.* **1982**, *236*, C45−C48 and references therein.

(33) Evans, D. H.; O'Connell, K. M.; Peterson, R. A.; Kelly, M. J. *J. Chem. Educ.* **1983**, *60*, 290−293.

(34) Mabbot, G. A. *J. Chem. Educ.* **1983**, *60*, 697−701.

(35) Low concentrations had to be employed to avoid polymerization on the electrode.

(36) Pedulli, G. F.; Todres, Z. V. *J. Organomet. Chem.* **1992**, *439*, C46−C48.

(37) The unusually large **g**-factor (2.0056 vs 2.00479 in the nitrobenzene radical anion) and the small hyperfine couplings ($a = 0.213$ G) to the protons in the 2-position of the ferrocen-1-yl unit also indicate some (very limited) delocalization of spin density onto the ferrocene donor.

(38) Gassman, P. G.; Macomber, D. W.; Hershberger, J. W. *Organometallics* **1983**, *2*, 1470−1472.

(39) Coe, B. J.; Jones, C. J.; McCleverty, J. A.; Bloor, D.; Cross, G. *J. Organomet. Chem.* **1994**, *464*, 225−232.

(40) Hoh, G. L. K.; McEwen, W. E.; Kleinberg, J. *J. Am. Chem. Soc.* **1961**, *83*, 3949−3953.

(41) Robbins, J. L.; Edelstein, N.; Spencer, B.; Smart, J. C. *J. Am. Chem. Soc.* **1982**, *104*, 1882−1893.

(42) Interestingly, the difference in ease of oxidation between **Fc″[1]2** (−270 mV vs ferrocenium/ferrocene) and the parent octamethylferrocene (−360 mV) is somewhat larger than that between **Fc[1]2** (+25 mV) and ferrocene (0 mV). This reflects the greater contribution of charge-transferred resonance structures to the ground state in the stronger donor (octamethylferrocenyl) case.

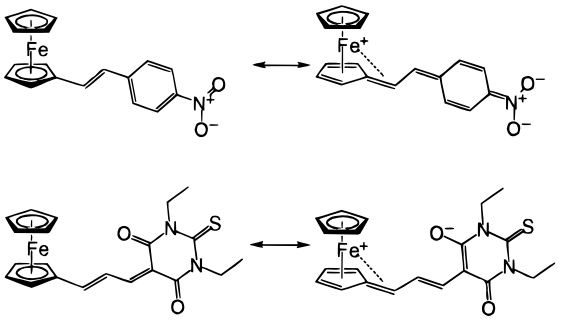

Figure 6. Neutral (left) and charge-transfer (right) resonance structures for **Fc[1]2** (top) and **Fc[2]5** (bottom).

conjugation length between donor and acceptor, changing iron for ruthenium or osmium, and varying degrees of methylation of the cyclopentadienyl rings. We will begin by briefly restating these models. In model I,[6] the LE transition is **M**→π***** and the HE transition is π→**A**. In model II,[18−20] the LE transition is d−d and the HE transition is **M**→A. In model III (the present model), the LE transition is **M**→**A** and the HE transition is π→**A**. The models are summarized diagrammatically in Figure 3.

(a) Effect of a Stronger Acceptor. All three models predict a red-shift of the HE transition on increasing acceptor strength, since in all three models this transition involves charge transfer to an empty acceptor-based orbital. However, the models disagree over the behavior of the LE transition. In model I, this is **M**→π*****; since π***** has only a small acceptor contribution, this transition is predicted to be relatively insensitive to acceptor strength. In model II the LE transition is a d−d ligand field transition; if it were a pure d−d transition it should be insensitive to acceptor strength. The observed variable energy of the LE transition and its large extinction coefficient (compared to that of a typical d−d transition) were previously attributed to borrowing of intensity from charge-transfer transitions via coupling through vibrational modes.[19] If this coupling is a minor perturbation then the description of the transition as a ligand-field transition remains valid. However, if the coupling is large it is necessary to account for this when describing the transition, which will become increasingly important as a contributor to the nonlinearity. Model III predicts a red-shift for the LE (**M**→**A**) transition of similar magnitude to that for the HE transition since both transitions involve charge transfer to the same empty orbital.

When the *p*-nitrophenyl acceptor (**Fc[1]2**) is replaced by a stronger acceptor such as *p*-*N*-methylpyridinium (**Fc[1]3-X**), or by an even stronger acceptor such as the 2-phenylthioflavone derivative shown in Figure 1 (**Fc[1]4-ClO$_4$**), *both* transitions show red-shifts of similar magnitude (1.04 and 0.99 eV red-shifts for HE and LE transitions, respectively, on moving from **Fc[1]2** to **Fc[1]4-ClO$_4$**), most consistent with model III (see Figure 2 in ref 12). Another comparison can be made by examining the spectra of **Fc[1]2** and **Fc[1]6** (Figure 7). Again the shifts are similar in magnitude (0.50 eV for the HE transition, 0.60 eV for the LE transition).[44] These shifts are also of similar magnitude to the difference of 580 mV between the [m]/[m]$^-$ potentials of the two compounds (vide supra). Furthermore, there

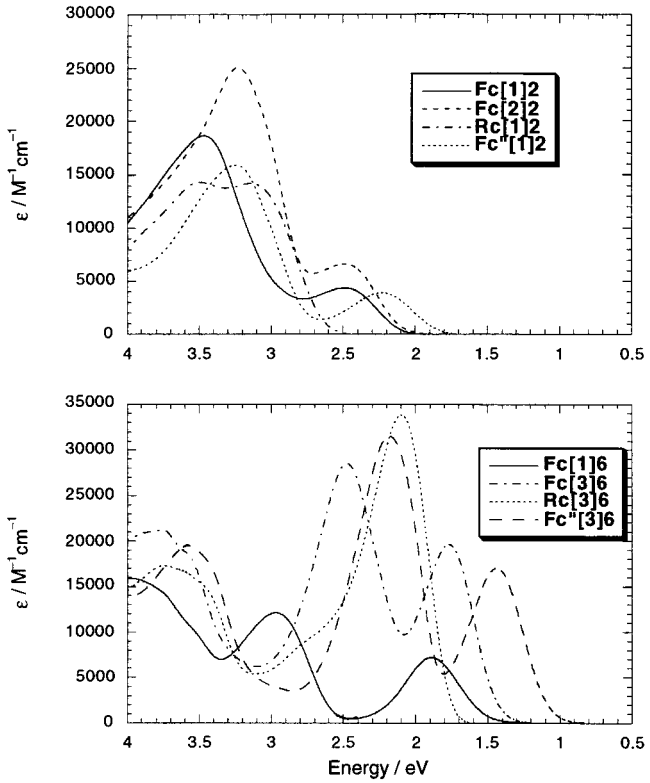

Figure 7. UV−vis spectra of metallocene chromophores containing nitrobenzene (**Mc[*n*]2** series) and 1-dioxothia-3-(dicyanomethylene)-indane (**Mc[*n*]6** series) acceptors in 1,4-dioxane.

is a marked tendency for the oscillator strength of the LE transition to increase relative to that of the HE transition with increasing acceptor strength. For example, in the series **Fc[1]2**, **Fc[1]3-Br**, and **Fc[1]4-ClO$_4$**, the oscillator strength for the LE transition changes from 0.10 to 0.11 to 0.25, while that for the HE transition decreases from 0.60 to 0.51 to 0.43.[12] The same effect is seen by comparing some of the compounds in Figure 7.[44] This is consistent with increased intensity borrowing in the stronger acceptor species; this arises from the increased mixing of states brought about by the lowering in energy of the two excited states (decrease in $\Delta E_{ge'}$). However, different spatial orbital extents, and therefore varying overlap with donor orbitals, of the LUMOs of the different acceptors may also be a contributory factor to the observed variations in intensities.

Toma and co-workers found that, although the LE transitions for a wide range of arylferrocenes[45] and 1-ferrocenyl-2-arylethylenes[22] were similar to the d−d transition of ferrocene itself[46] and showed a weak dependence upon the Hammett parameters of the substituents, the LE transitions of derivatives with strongly electron-withdrawing substituents (*p*-CHO, *p*-CN, and *p*-NO$_2$) could not readily be correlated with Hammett parameters. Thus, their data suggest the LE transitions of the strong acceptor compounds are not typical d−d transitions, consistent with the present hypothesis (model III) that they are better described as charge-transfer transitions.

(b) Effect of a Longer Conjugated Bridge. Simple Hückel arguments predict that an increase in conjugation length will

(43) Evidence for the contribution of this type of resonance structure may be found in the ^{1}H NMR spectra of species with strong acceptors, where ^{1}H−^{1}H couplings across formally double C−C bonds are reduced. Thus, in the strong acceptor compounds **Fc″[3]5** and **Fc″[3]6** ^{1}H−^{1}H coupling constants of ca. 13 Hz (in CD_2Cl_2) are seen across both single and double bonds, whereas, in the parent aldehyde, Fc″(CH=CH)$_2$CHO, the coupling constants alternate between ca. 15 Hz for formally double bonds and ca. 10 Hz for formally single bonds (C_6D_6).

(44) The two molecules in this comparison have somewhat different π-bridges and consequently the orbitals π are not so comparable as in the **Fc[1]2**/**Fc[1]4-ClO$_4$** comparison; therefore, it is not surprising that the two bands do not show as similar shifts to one another as in that comparison.

(45) Toma, S.; Gáplovsky, A.; Hudecek, M.; Langfelderová, Z. *Monatsh. Chem.* **1985**, *116*, 357−364.

(46) Sohn, Y. S.; Hendrickson, D. N.; Gray, H. B. *J. Am. Chem. Soc.* **1971**, *93*, 3603−3612.

lead to an increase in the energy of the highest occupied orbitals associated with the π-backbone and a decrease in the lowest unoccupied π-backbone orbitals. Metallocene- and acceptor-localized orbitals should be little affected by the nature of the conjugated bridge. Thus, in model I, the lowering of π^* will lead to a red-shift of the LE transition, while the raising of π will red-shift the HE transition. Model II predicts the energies of both transitions will be only weakly affected by the change in conjugation length as the LE and HE transitions involve substantially metal-localized orbitals or metal- and acceptor-localized orbitals, respectively. In model III, as in model I, the combination of e_1' and π-bridge orbitals (π, HOMO-3), should rise in energy with increased conjugation length. Thus, the HE transition is expected to red-shift, while the energy of the LE transition, involving only metal- and acceptor-localized orbitals, should be insensitive to conjugation length.

The experimental results are best explained with use of model III. We have previously compared spectra for the **Fc[n]6** series (see Figure 2 in ref 12); those for **Fc[1]6** and **Fc[3]6** are also shown in Figure 7, together with those for **Fc[1]2** and **Fc[2]2**. The HE transition of **Fc[n]6** red-shifts by ca. 0.70 eV as n is increased from 1 to 4. The LE transition is much less sensitive to chain length, the small variation (0.22 eV) observed between the extreme cases probably reflecting deviation from the idealized model, i.e., in molecules with stronger acceptors **A** can mix more strongly with π-levels. Excepting **Fc[4]6**, both transitions are observed to increase in intensity with increasing chain length. It is well-known that the intensity of polyene $\pi-\pi^*$ transitions increases with chain length.[47] The increase in intensity of the low-energy transition may also reflect increased intensity borrowing, owing to the decreased separations ($\Delta E_{ge'}$, $\Delta E_{ee'}$) between states. The intensity of both transitions of α,ω-diferrocenylpolyenes has also been found to increase with increasing chain length.[48,49]

(c) Effect of Exchanging Fe for Ru. The first ionization potential of ruthenocene is substantially greater than that of ferrocene.[27−29] The e_1' cyclopentadienyl orbitals (which combine with polyene bridge orbitals to give the HOMO-3, labeled π, in models I and III) of ruthenocene are, however, quite similar in energy to those of ferrocene. The acceptor orbitals should also be insensitive to the identity of the metallocene; the reduction potentials in Table 3 support this hypothesis. Hence, model I predicts a blue shift for the **M**→π^* LE transition, while the higher energy π→**A** transition should be only slightly blue-shifted from that of the corresponding ferrocene analogue. Model II predicts that both transitions will undergo large blue-shifts: the LE transition due to the greater ligand field splittings characteristic of the heavier transition metals (indeed, the lowest energy spin-allowed d−d transition of ruthenocene is blue-shifted by 0.96 eV relative to that of ferrocene[46]), and the HE transition due to the higher ionization energy of ruthenocene. In the case of exchanging Fe for Ru, model III makes equivalent predictions to model I.

Experimentally, the LE transition is blue-shifted by ca. 0.3 to 0.6 eV, while the HE transition is shifted by less than 0.2 eV. In molecules with fairly weak acceptors, such as nitrophenyl, to which model III is most successfully applied, the blue shift of the LE transition is comparable with that expected by comparing first IEs of either the parent metallocenes or the dyes themselves. Thus, in **Rc[1]2** the LE transition (in *p*-dioxane) is blue-shifted by ca. 0.65 eV relative to **Fc[1]2** (Figure 7); the ionization potentials of the parent metallocenes differ by 0.57 eV. Other comparisons of spectra may be found in refs 5, 11, and 12. Also noteworthy is the dramatic increase in the intensity of the LE transition at the expense of that of the HE transition when iron is exchanged for ruthenium. One factor is presumably that the decreased energy difference between **M** and π levels, and thus decreased $\Delta E_{ee'}$, leads to increased mixing of first and second excited states, and thus increased intensity borrowing by the nominally **M**→**A** transition from the π→**A** transition. A second factor may be the increased d-orbital extent of ruthenium, leading to increased direct or indirect spatial overlap with **A**. Evidence for this increased extent may be found in the crystal structures of metallocenyl carbocations; ruthenocenyl compounds are best described as [(η^6-fulvene)(η^5-cyclopentadienyl)ruthenium] cations,[50,51] while the corresponding iron compounds are perhaps best regarded as distorted ferrocenes.[52,53] For *E*-1-osmocenyl-2-(*p*-nitrophenyl)ethylene, **Oc[1]2**, only a single transition is observed, at similar energy to the HE transition of its iron and ruthenium analogues; presumably the blue-shift of the LE transition is sufficiently large that the two transitions overlap in this case.

(d) Effect of Metallocene Methylation. Methylation of both metallocene cyclopentadienyl rings (**Fc″** derivatives) will raise the energy of both the metal d-orbitals and the highest filled π orbitals, as evidenced by comparison of the photoelectron spectra of ferrocene and decamethylferrocene.[28] Model I predicts the HE (π→**A**) transition will red-shift on replacing a metallocene with the corresponding methylated metallocene; the effect on the LE transition depends on the relative magnitudes of the effects of methylation on **M** and π^*. Model II also predicts a red-shift for the HE (**M**→**A**) transition, but a *blue*-shift for the LE (d−d) transition on methylation; methylated cyclopentadienyl ligands are known to lead to *greater* ligand-field splittings than their unmethylated analogues.[41,54] Model III predicts red-shifts for both transitions; both donor levels will be raised in energy, while the common acceptor level will be unchanged. The predictions are broadly similar for the case of methylating the cyclopentadienyl ring not bearing the π-bridge (**Mc′** derivatives), the details of the predictions for models I and III depending on the Cp* orbital contribution to π.

We have previously reported UV−vis absorption maxima for the 1′,2′,3′,4′,5′-pentamethylmetallocen-1-yl derivatives, **Fc′[1]2** and **Rc′[1]2**.[6] In the iron case, shifts of 0.095 and 0.17 eV were observed relative to the unmethylated analogue for the high- and low-energy transitions, respectively, while in the ruthenium case, shifts of 0.19 and 0.23 eV were found. In the new compound **Fc″[1]2**, containing the 2,3,4,5,1′,2′,3′,4′-octamethylferrocen-1-yl group, the shifts are 0.21 and 0.26 eV for high- and low-energy transitions, respectively (see Figure 7). Interestingly, the shift of the energy of the low-energy transition of the ferrocene compound observed with eight methyl groups

(47) Klessinger, M.; Michl, J. *Excited States and Photochemistry of Organic Molecules*; VCH: New York, 1995.

(48) Ribou, A. C.; Launay, J.-P.; Sachtleben, M. L.; Li, H.; Spangler, C. W. *Inorg. Chem.* **1996**, *35*, 3735−3740.

(49) A related issue is that of *E*/*Z* isomerism. On moving from **Fc[1]2** (*E*) to **Fc[1]1** (*Z*), a blue shift of 0.33 eV is found for the HE UV−vis−NIR transition, for which we propose the planarity dependent cyclopentadienyl/nitrostyrene combination (π, HOMO-3) as donor, while the LE transition blue shifts by only 0.08 eV, consistent with a transition originating from the metal $d_{z^2}/d_{x^2-y^2}/d_{xy}$ orbitals (**M**), which are unaffected by the bridge planarity. These results are also consistent with the UV−PES data for **Fc[1]1** and **Fc[1]2**.

(50) Kreindlin, A. Z.; Petrovskii, P. V.; Rybinskaya, M. I.; Yanovskii, A. I.; Struchkov, Y. T. *J. Organomet. Chem.* **1987**, *319*, 229−237.

(51) Sato, M.; Kudo, A.; Kawata, Y.; Saitoh, H. *Chem. Commun.* **1996**, 25−26.

(52) Cais, M.; Dani, S.; Herbstein, F. H.; Kapon, M. *J. Am. Chem. Soc.* **1978**, *100*, 5554−5558.

(53) Sime, R. L.; Sime, R. J. *J. Am. Chem. Soc.* **1974**, *96*, 892−896.

(54) Robbins, J. L.; Edelstein, N. M.; Cooper, S. R.; Smart, J. C. *J. Am. Chem. Soc.* **1979**, *101*, 3853−3857.

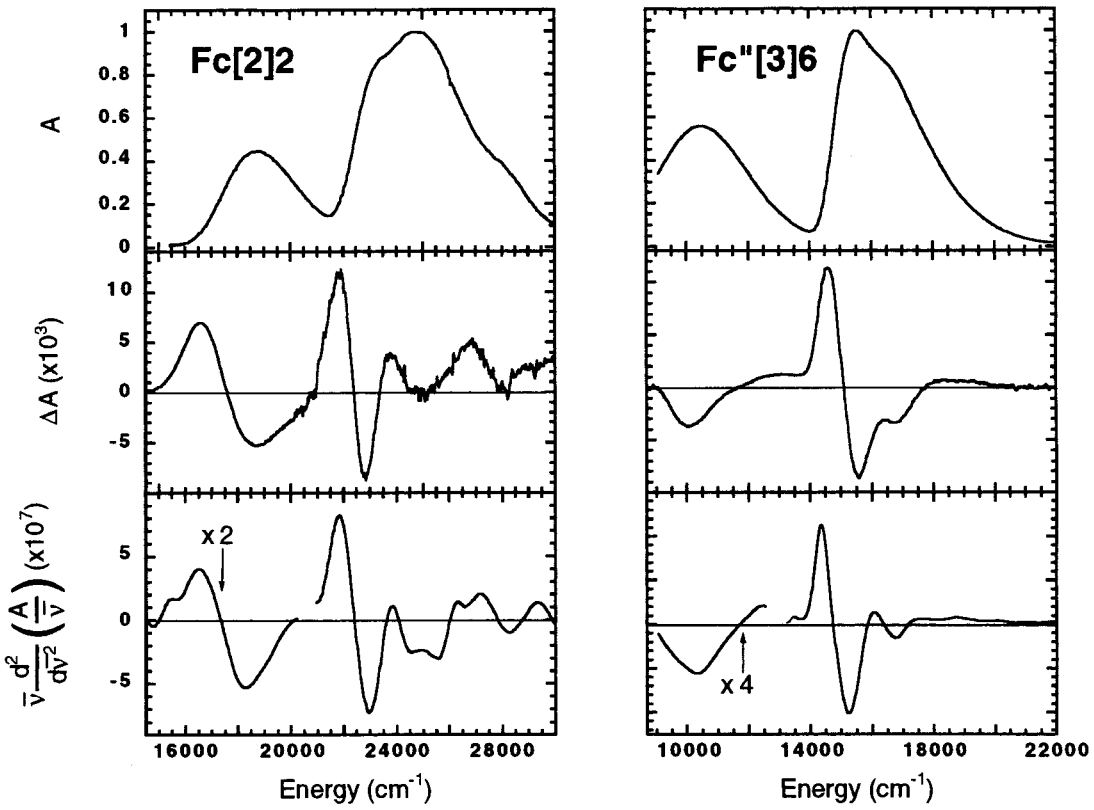

Figure 8. Absorption spectra (top panels), Δ*A* (Stark) spectra (center panels), and $\bar{\nu}$-weighted second derivatives of the absorption spectra (bottom panels) for **Fc[2]2** (left) and **Fc″[3]6** in frozen 2-methyltetrahydrofuran. The absorption of the samples was scaled so both are equal to unity at the absorption maximum and for an applied field strength of 1 MV cm^{-1} in order to facilitate comparisons. The second derivatives of the low-energy bands have been multiplied by factors of 2 and 4, respectively, to simulate their importance in the Stark spectra.

is ca. 8/5 times that observed with five methyl groups. This is in accordance with the well-documented additive effect of alkyl groups upon ferrocene oxidation potentials[38,40] and is entirely in agreement with the present model of a donor orbital resembling that of the parent metallocene and an acceptor orbital relatively unaffected by the metallocene. The shift in the high-energy transition with eight methyl groups is, however, ca. 2.2 times that with five methyl groups. This reflects the greater contribution of the cyclopentadienyl ring directly bound to the π-bridge (methylated in the octamethyl compound, unmethylated in the pentamethyl example) to the HOMO-3, π. Shifts of similar magnitude are also seen in octamethylated species with longer π-bridges and stronger acceptors (Figure 7). These results appear to exclude the possibility that the low-energy transition is a d−d transition. Of course, it may be argued that sufficient charge-transfer character is mixed into the transition such that the lower charge-transfer energy expected on methylation outweighs the higher ligand-field splitting, but if this is the case, then the transition is more appropriately described in terms of a charge-transfer transition.

In summary, the present model (model III) is best able to account for the effects of structural changes upon the transition energies and intensities.

Solvatochromism and Stark Spectroscopy. The three models make different qualitative predictions about the dipole moment changes, $\Delta\mu$, associated with the two transitions in the neutral dyes. Charge transfer (**M**→**A**, **M**→π*, π→**A**) transitions are expected to be associated with large $\Delta\mu$ values. For a ligand-field transition, however, the charge redistribution is spatially very limited and, therefore, $\Delta\mu$ will be small.

Both transitions in the UV−vis−NIR of all the neutral metallocene−bridge−acceptor molecules considered in this paper show positive solvatochromism (cationic species such as **Mc[*n*]4-X**[12] show negative solvatochromism, since in these species the ground-state dipole moments are opposite in sign to those of the neutral species, due to the acceptor-localized positive charges, but the charge transfer is in the same direction as in the neutral species). The LE and HE transitions of **Fc[1]2** show bathochromic shifts of 0.16 and 0.23 eV, respectively, on moving from heptane to DMF.[4] For **Fc″[3]6**, red-shifts of 0.11 and 0.30 eV are seen for LE and HE energy transitions, respectively, between cyclohexane and DMSO.[55] Analogous solvatochromism has previously been reported for a variety of ferrocene donor−acceptor compounds with different types of π-bridges or acceptors.[8,39,56] Positive solvatochromism is generally taken as an indication of an increase in dipole moment with photoexcitation; thus, solvatochromism of both bands is consistent with both models I and III. In principle, $\Delta\mu$ can be estimated from solvatochromism data by using the McRae equation;[57] however, the analysis requires assumptions to be made about molecular shape. Some other problems of this type of analysis have recently been discussed.[58]

Electroabsorption, or Stark spectroscopy, of frozen solutions provides an alternative method to determine $|\Delta\mu|$; the method, its application to merocyanine dyes, and its limitations have recently been discussed.[59] Frozen 2-methyltetrahydrofuran solu-

(55) Spectra showing the solvatochromism of **Fc″[3]6** are presented in the Supporting Information.

(56) Houlton, A.; Jasim, N.; Roberts, R. M. G.; Silver, J.; Cunningham, D.; McArdle, P.; Higgins, T. *J. Chem. Soc., Dalton Trans.* **1992**, 2235−2241.

(57) McRae, E. G. *J. Phys. Chem.* **1957**, *61*, 562−572.

(58) Lombardi, J. R. *J. Phys. Chem. A* **1998**, *102*, 2817−2823.

(59) Bublitz, G. U.; Ortiz, R.; Marder, S. R.; Boxer, S. G. *J. Am. Chem. Soc.* **1997**, *119*, 3365−3376.

tions of **Fc[2]2** and **Fc″[3]6** were investigated by Stark spectroscopy; Figure 8 shows the absorption spectra, Stark spectra, and the $\bar{\nu}$-weighted second derivatives of the absorption spectra. In both cases the Stark spectra show overall second-derivative line shapes. First-derivative contributions to Stark spectra arise from polarizability changes, $\Delta\alpha$, associated with transitions; second-derivative contributions reflect dipole moment changes, $|\Delta\mu|$, associated with transitions. In the figure, the second derivatives of the LE transitions have been multiplied by factors of 2 or 4 for **Fc[2]2** and **Fc″[3]6**, respectively, in order to replicate the relative magnitudes of the two transitions in the appropriate Stark spectra. The result indicates that, for each compound, a larger dipole moment change is associated with the LE transition. For **Fc[2]2**, $|\Delta\mu|$ for the LE transition is ca. $\sqrt{2}$ times that of the HE transition, while $|\Delta\mu|$ for the LE transition of **Fc″[3]6** is approximately twice that for the HE transition. For **Fc″[3]6**, the data quality allowed quantitative anlaysis: $|\Delta\mu|$ for the LE is ca. 18 D, that for the HE transition is ca. 9 D.

The observation of large dipole moment changes of similar magnitude for *both* transitions indicates *both* transitions have considerable charge-transfer character. Moreover, given the relative transition energies and transition dipole moments, large $|\Delta\mu|$ terms for both transitions mean that both transitions will make significant contributions to the observed values of β. The relative two-level contributions can be estimated according to eq 1. For **Fc[2]2**, 63% of the two-level contribution is from the HE transition, while the LE transition contributes 37%. For **Fc″[3]6**, the HE transition is responsible for ca. 25% of the two-level contributions, while the LE transition contributes 75%. Assuming the validity of the two-level model, these results demonstrate, *independently of the spectral assignment*, that *both* transitions make contributions of comparable magnitude to the observed optical nonlinearity.

Summary

We have described a simple orbital model (model III) for understanding the spectra of metallocene−(π-bridge)−acceptor NLO-chromophores. We have tested the model by making qualitative predictions about the dependence of the UV−vis−NIR spectra of these molecules upon changes in chromophore structure; these predictions are in better agreement with experiment than the predictions of two previously published models.[6,19] While none of the models is adequate to explain all the data for the wide range of compounds considered, UV−PES, DF calculations, and cyclic voltammetry are generally consistent with model III. Stark spectroscopy confirms that large dipole moment changes are associated with both low-energy transitions in these molecules; together with the energies and intensities of the transitions, this indicates that the two transitions make comparable contributions to the observed nonlinear optical properties. Although there is still room for improvement in model III, it is more robust in its predictive capabilities than the previous models and should, therefore, be a helpful guide to chemists seeking to intuitively understand the spectroscopy and NLO responses of this class of molecules.

Acknowledgment. Support from the National Science Foundation (Chemistry Division), Office of Naval Research, Air Force Office of Scientific Research (AFOSR) at Caltech is gratefully acknowledged. The research described in this paper was performed in part by the Jet Propulsion Laboratory (JPL), California Institute of Technology, as part of its Center for Space Microelectronics Technology and was supported by the Ballistic Missile Defense Initiative Organization, Innovative Science and Technology Office through an agreement with the National Aeronautics and Space Administration (NASA). Support from the North Atlantic Treaty Organization (NATO) Grant No. 910903 is also gratefully acknowledged. Work at Stanford was supported in part by grants from the NSF Chemistry Division. H.E.B. thanks the Science and Engineering Research Council (SERC) for a studentship. We thank Arjun Mendiratta for technical assistance and Professors S. Toma, H. B. Gray, and M. Ratner for helpful comments.

Supporting Information Available: Experimental details for synthesis of new compounds, instrumental methods, and DF calculations. He(I) and He(II) PE spectra for *p*-nitrostyrene, **Fc[1]1**, **Fc[1]2**, **Rc[1]1**, and **Oc[1]2**; figure comparing cyclic voltmmograms of **Fc″[1]2**, octamethylferrocene and nitrobenzene; figure illustrating solvatochromism of **Fc″[3]6** (PDF). This material is available free of charge via the Internet at http://pubs.acs.org.

JA9830896